Chinese Journal of Polymer Science Vol. 35, No. 2, (2017), 302−308

Chinese Journal of Polymer Science

Efficient P3HT:$PC_{61}BM$ Solar Cells Employing 1,2,4-Trichlorobenzene as the Processing Additives*

Wei-chao Chen[a, b], Man-jun Xiao[a], Chun-peng Yang[a**], Lin-rui Duan[a] and Ren-qiang Yang[a**]
[a] *Chinese Academy of Sciences Key Laboratory of Bio-based Materials, Qingdao Institute of Bioenergy and Bioprocess Technology, Chinese Academy of Sciences, Qingdao 266101, China*
[b] *College of Textiles & Clothing, Qingdao University, Qingdao 266071, China*

Abstract The efficiency of the poly(3-hexylthiophene) (P3HT) and [6,6]-phenyl C_{61}-butyric acid methyl ester ($PC_{61}BM$) based organic solar cells was enhanced by using 1,2,4-trichlorobenzene (TCB) as a processing additive to control the blend morphology. The addition of TCB improved the arrangement of P3HT which resulted in good phase separated blend films. Correspondingly, the optimized solar cells showed a power conversion efficiency (PCE) of 4.17% with a fill factor (FF) of 0.69, which were higher than those of common thermal annealing devices (PCE 3.84%, FF 0.67). The efficiency was further improved to 4.74% by thermal annealing at 150 °C for 10 min with a higher FF of 0.74.

Keywords Organic solar cells; Crystallinity; Additive; Morphology

INTRODUCTION

Organic solar cells (OSCs) based on polymer-fullerene bulk heterojunction have attracted much attention due to their potential advantages, such as light-weight, flexibility and low-cost manufacturing[1−8]. The power conversion efficiency (PCE) of solution processed OSCs has rapidly increased to over 9% for single and 11.5% for tandem junction devices[9−11], which was ascribed to the development of novel semiconducting polymers and the appropriate morphological control methods. Apparently, for the improvement of PCE, it is crucial to design suitable semiconducting polymers which possess a wide absorption range and appropriate energy levels favoring for exciton separation and high photovoltage[7, 12]. Meanwhile, the optimization of the bulk heterojunction (BHJ) blend morphology is another important factor for highly efficient solar cells[13, 14]. A bicontinuous interpenetrating network with suitable phase separation size is important for the exciton separation, charge carrier transport and collection.

In order to control blend morphologies, many methods have been explored to prepare active layer. Thermal annealing treatment is the most commonly used method to modulate phase separation in polymer-fullerene blend films[15, 16]. In P3HT:$PC_{61}BM$ blend film, annealing could improve the crystallinity of P3HT, and drive the separation of P3HT and fullerenes, finally form bicontinuous interpenetrating network. Besides, other methods are also effective to control morphologies. For example, solvent annealing has been used to control phase separation in P3HT:$PC_{61}BM$ blends[17−19]; controlling evaporation rate of the residual solvent also generates a

* This work was financially supported by the National Natural Science Foundation of China (Nos. 61405209 and 51573205).
** Corresponding authors: Chun-peng Yang (杨春鹏), E-mail: yangcp@qibebt.ac.cn
Ren-qiang Yang (阳仁强), E-mail: yangrq@qibebt.ac.cn
Invited paper for special issue of "Opto-electronic Functional Polymer"
Received October 14, 2016; Revised November 8, 2016; Accepted November 10, 2016
doi: 10.1007/s10118-017-1892-y

bicontinuous interpenetrating network. Compared to the above mentioned methods, processing additive is a relatively simple approach in the pursuit of improved BHJ morphology without conventional annealing processes.

The pioneering work by Peet *et al.* showed that introducing 1,8-octanedithiol as a processing additive improved the morphology of the BHJ layer, leading to an increased efficiency of the OSC[20]. Later, different additives have been employed in different polymer:$PC_{61}BM$ systems. Consistently, higher PCEs for many systems were obtained by using additive[9, 21–24]. Theoretically, in this method, the key to success is the selection of appropriate additive for different systems[25, 26].

P3HT, a typical organic semiconducting material, has been investigated extensively in the field of organic solar cells. Different additives have been tried in the P3HT:$PC_{61}BM$ system[27–32]. The devices based on P3HT:$PC_{61}BM$ showed good performance without annealing, since the organization of P3HT was improved by additives during coating.

In this work, highly efficient P3HT:$PC_{61}BM$ solar cells were fabricated using chlorobenzene (CB) as the host solvent and 1,2,4-trichlorobenzene (TCB) as the processing additive. The addition of TCB enhanced the ordering of P3HT, and a good interpenetrating network was formed without annealing. The devices exhibited a PCE of 4.17% and a high FF of 0.69, which were higher than those of common thermal annealing devices without additives (PCE 3.84%, FF 0.67). The PCE was further improved to 4.74% after annealing and the FF reached up to 0.74.

EXPERIMENTAL

P3HT was purchased from Lumtec and $PC_{61}BM$ was obtained from American Dye Sources (ADS). Patterned ITO glass with a sheet resistance of 15 Ω per square was obtained from Shenzhen Display (China). All of these commercially available materials were used as received without further purification.

The solar cells were prepared with the structure ITO/PEDOT:PSS/P3HT:$PC_{61}BM$/Ca/Al. Patterned ITO-coated glass was cleaned with ITO detergent, deionized water, acetone and isopropanol in an ultrasonic bath for 20 min each time, and then exposed to oxygen plasma for 6 min. PEDOT:PSS (Baytron P VP Al 4083) was spin-coated onto ITO-coated glass substrates, followed by annealing at 160 °C for 30 min. Subsequently, the substrates were transferred to a glovebox. The active layers were prepared by spin coating (600 $r \cdot min^{-1}$) the solution of P3HT and $PC_{61}BM$ onto the ITO coated glass for 1 min. The weight ratio of P3HT:$PC_{61}BM$ was 1:1, and the total concentration was 36 $mg \cdot mL^{-1}$ in CB with different ratio TCB. The active layers were annealed at 150 °C for 10 min. Finally, after the samples were transferred to a vacuum chamber, Ca (10 nm) and Al (100 nm) were deposited *via* a mask to define the active area of 0.10 cm^2 in high vacuum.

Atomic force microscopy (AFM) measurements of film morphology were imaged by an Agilent 5400 with tapping mode. The out-of-plane X-ray diffraction (XRD) patterns were taken from a D8 ADVANCE discovery thin-film diffractometer. The in-plane GIXD measurements were carried out at shanghai Synchrotron Radiation Facility (SSRF). TEM images were obtained on a JEOL JEM-1011 transmission electron microscope at an accelerating voltage of 100 kV.

PCE was calculated from current density-voltage (*J-V*) curves which were recorded by a Keithley 2420 source meter under illumination of an AM1.5G solar simulator with an intensity of 100 $mW \cdot cm^{-2}$. The light intensity was determined by a standard silicon photodiode. EQEs were measured using a Newport 2931-C coupled with the 300 W Xenon lamp.

RESULTS AND DISCUSSION

The *J-V* curves of the devices with different ratios of TCB as the additive measured under AM1.5G irradiation at 100 $mW \cdot cm^{-2}$ are shown in Fig. 1. The common thermal-annealing devices without TCB are also included for comparison. The parameters of the devices are summarized in Table 1. The control devices without additive and thermal annealing show poor photovoltaic performances with a low short-circuit current density (J_{sc}) of 2.41 $mA \cdot cm^{-2}$ and a FF of 0.51, which may be caused by the poor interpenetrating network in P3HT:$PC_{61}BM$

blend film[33]. However, when 1% TCB is added, the device shows a J_{sc} of 6.09 mA·cm^{-2} and a high FF of 0.66. Upon further increasing the ratio of TCB from 2% to 4%, all the devices exhibit high FF (over 0.66) and J_{sc}. The optimized PCE of 4.17% is obtained with FF = 0.69 and J_{sc} = 9.91 mA·cm^{-2} when adding 3% TCB without annealing. Meanwhile, the open-circuit voltage (V_{oc}) keeps almost the same (0.61 V) regardless of thermal-annealing. All the PCEs of the devices with TCB from 2% to 4% are higher than the control device with thermal-annealing (3.84%). The results indicate that TCB is an effective processing additive for improving PCE.

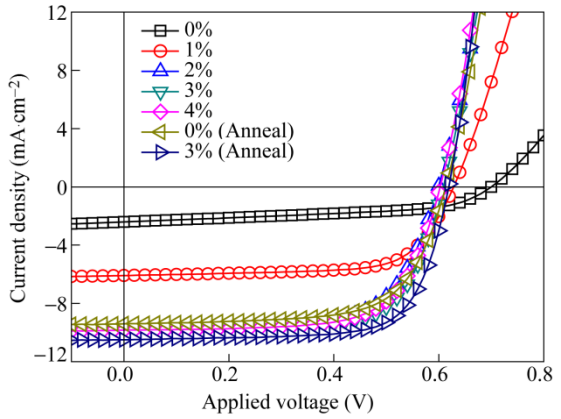

Fig. 1 *J-V* curves of P3HT:PC$_{61}$BM solar cells with different TCB ratios

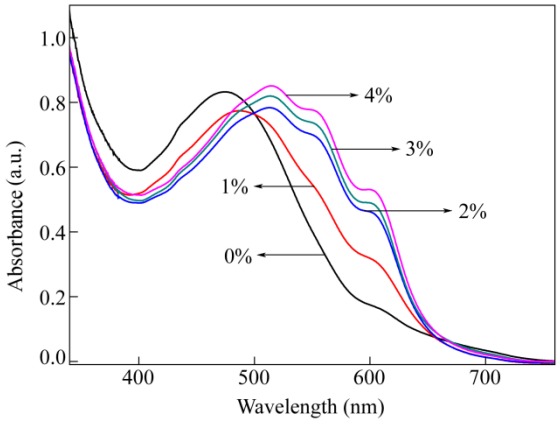

Fig. 2 The absorption spectra of P3HT:PC$_{61}$BM films with different TCB ratios

Table 1 The parameters of the devices based on P3HT:PC$_{61}$BM with different ratios of TCB

	V_{oc} (V)	J_{sc} (mA·cm^{-2})	FF	PCE (%)	PCE$_{ave}$ [a] (%)
0% TCB	0.70	2.41	0.51	0.86	0.80
1% TCB	0.63	6.09	0.66	2.53	2.43
2% TCB	0.60	9.76	0.67	3.92	3.85
3% TCB	0.61	9.91	0.69	4.17	4.09
4% TCB	0.60	9.83	0.67	3.95	3.83
0% TCB (Anneal)	0.61	9.40	0.67	3.84	3.76
3% TCB (Anneal)	0.61	10.50	0.74	4.74	4.65

[a] The average PCE was obtained from 10 devices.

The absorption spectra of P3HT:PC$_{61}$BM films with different ratios of TCB were investigated and are shown in Fig. 2. The film without additive exhibits a typical absorption spectrum similar to the reported ones[16, 17]. On the contrary, the films with additive (≥ 2%) show wider absorption range and exhibit three featured absorption peaks. One peak is at *ca.* 520 nm, which is corresponding to the π-π^* transition, and the two vibronic shoulders are at *ca.* 550 nm and 610 nm, which is an expression of strong interchain-interlayer interaction or high crystallinity of P3HT[16, 17, 29]. This result indicates that the addition of TCB in the blend film enhances the ordering of P3HT phase. Obviously, the independent position of absorption peaks and the gradually increased absorption intensity with TCB ratio increasing from 2% to 4% also demonstrated that the addition of TCB could improve the organization of P3HT in the blend films.

To further verify the enhanced organization of P3HT in the blend films with different additives, out-of-plane X-ray diffraction was carried out on the films. The results are shown in Fig. 3. All the films showed an evident peak at 5.5° which is assigned to the (100) lattice plane of the P3HT[16]. On the other hand, the films with TCB additive present relatively stronger peak than the one without an additive, and the intensity of the diffraction peak increases with the ratio of TCB. The in-plane GIXD images are also shown in Fig. 3. The appearance of (300) lattice plane of P3HT in films with 3% TCB but not in films without TCB also certify the improvement of the crystallinity of P3HT. These further indicate that the crystallinity of P3HT was indeed

improved due to the additive of TCB, consistent well with the absorption spectra.

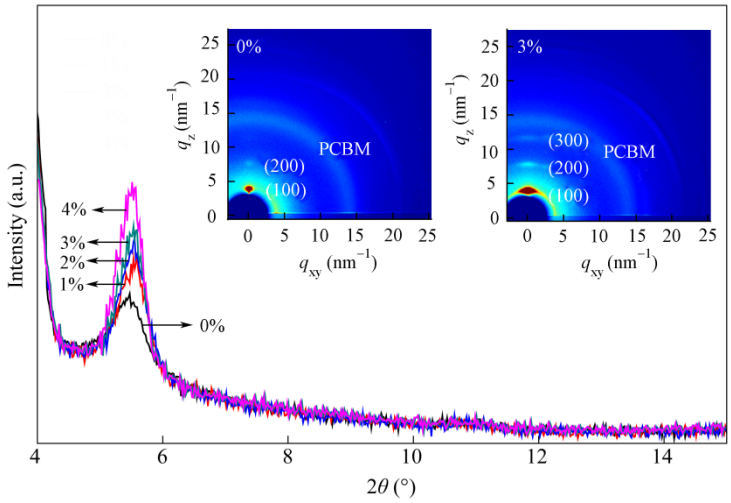

Fig. 3 Out-of-plane XRD of P3HT:$PC_{61}BM$ films with different TCB ratios and the insets are in-plane GIXD images of the films with 0% and 3% TCB

Figures 4(a)–4(e) show the atomic force microscopy (AFM) images of the films with different ratios of additive (0%–4%). The films without additive show smooth surface with a root-mean-square roughness (RMS) of 1 nm. However, the addition of TCB obviously raises RMS of the films to: 2.3 nm for 1% TCB, 8.2 nm for 2% TCB, 9.5 nm for 3% and 10.2 nm for 4%. Further, the domain sizes also increase by increasing the ratio of TCB. The rough surface may be caused by improvement of P3HT organization due to the addition of TCB[17]. Typical TEM images for films without TCB and with 3% TCB are shown in Figs. 4(g) and 4(h). The fibrillar P3HT crystals, which could be found (Fig. 4h) in the films with 3% TCB, further indicate that the crystallinity has been improved compared to the films without TCB. The increase of RMS could improve contact area between the electrode and the active layer, which would be beneficial for the collection of the charge carrier and thus increase the J_{sc}[17] .

The external quantum efficiency (EQE) curves of the devices are shown in Fig. 5. The curves are consistent with the absorption spectra of the films. The device without additive and annealing shows low and narrow light response, but, with the additive of TCB, light response increases gradually. The highest EQE value obtained is over 68%. The optimal current density obtained by integrating the EQE curve with the standard solar spectrum (AM1.5G) was 9.76 mA·cm^{-2}, which is well consistent with the measured value (about 9.91 mA·cm^{-2}) with small error (< 5%).

Effect of thermal annealing on the solar cell with 3% TCB is investigated. The *J-V* curve is shown in Fig. 1 and the corresponding parameter in Table 1. The device shows higher J_{sc} (10.50 mA·cm^{-2}) and FF (0.74) after annealing at 150 °C for 10 min and the PCE reaches up to 4.74%. The surface morphology of the films after thermo-annealing is shown in Fig. 4(f), which is similar to the films without thermo-annealing (Fig. 4d). This predicts that the structure of the films with 3% TCB may be relatively thermostable, which is very beneficial for the commercial process. One of the main factors that determine FF is the transport of charge carriers[2, 34]. The carrier mobility in the P3HT:$PC_{61}BM$ devices before and after annealing with 3% TCB was investigated by using trap-free space-charge-limited-current (SCLC) model[35]. The *J-V* curves of the diodes with the structures of ITO/PEDOT/P3HT:$PC_{61}BM$/Au for hole and ITO/ZnO/P3HT:$PC_{61}BM$/Ca/Al for electron are shown in Fig. 6 and the calculated hole (μ_h) and electron (μ_e) mobility are shown in Table 2. The films with and without annealing show almost the same hole mobility. However, compared with the film without annealing, the annealing one presents higher electron mobility, which leads to a lower ratio (μ_h/μ_e) between the hole and electron mobility (1.44 versus 1.86), indicating a more balanced carrier transport in the annealing films[17]. This is assumed to be the major reason for the high FF in the devices.

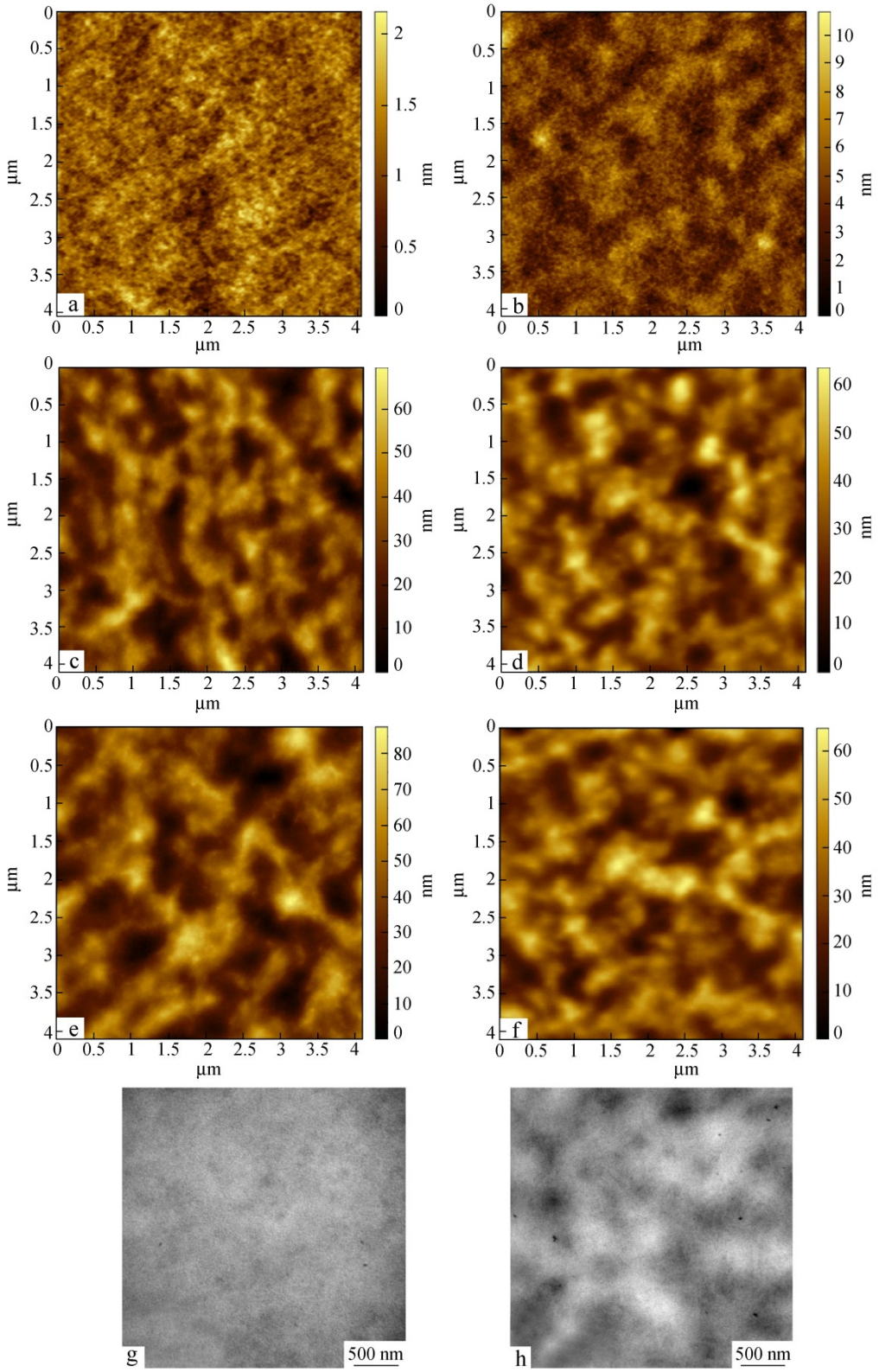

Fig. 4 AFM images (4 µm × 4 µm) of the films with different TCB ratios (a: 0% TCB, b: 1% TCB, c: 2% TCB, d: 3% TCB, e: 4% TCB, f: 3% TCB after thermo-annealing) and TEM images of the films with (g) 0% TCB and (h) 3% TCB

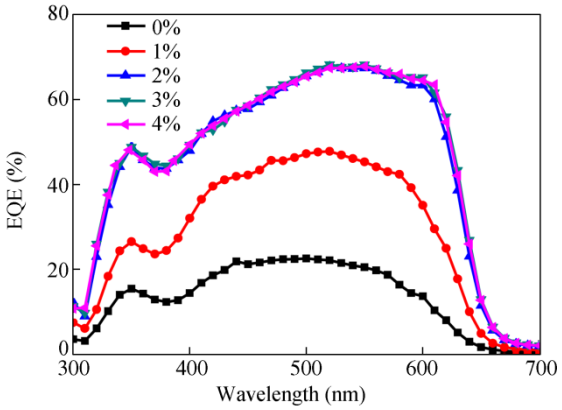

Fig. 5 EQE curves of P3HT:$PC_{61}BM$ solar cells with different TCB ratios

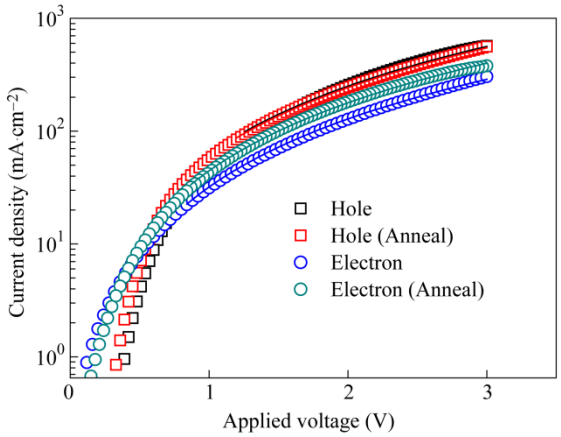

Fig. 6 *J-V* curves of ITO/PEDOT/P3HT:$PC_{61}BM$/Au diodes for hole and ITO/ZnO/P3HT:$PC_{61}BM$/Ca/Al diodes for electron (The online version is colorful.)
The symbols are experimental data for transport of holes and electrons respectively, and the solid lines are fitted according to the space-charge-limited-current model.

Table 2 The hole and electron mobility of P3HT:$PC_{61}BM$ films with 3% TCB before and after annealing

	μ_h ($cm^2 \cdot V^{-1} \cdot S^{-1}$)	μ_e ($cm^2 \cdot V^{-1} \cdot S^{-1}$)	μ_h/μ_e
3% TCB	1.60×10^{-3}	8.59×10^{-4}	1.86
3% TCB (Anneal)	1.70×10^{-3}	1.18×10^{-3}	1.44

CONCLUSIONS

In summary, highly efficient solar cells based on P3HT:$PC_{61}BM$ were fabricated by adding the processing additive TCB into the blend without annealing. The device shows the PCE of 4.17% and FF of 0.69, which are probably resulted from the high arrangement of P3HT induced by TCB. Besides, the PCE can be further improved to 4.74% with a J_{sc} of 10.50 mA·cm^{-2} and FF of 0.74. The high FF originates from the high charge carrier mobility and the good balanced carrier transport in the P3HT:$PC_{61}BM$ blend films.

ACKNOWLEDGMENTS The authors thank beamline BL14B1 (Shanghai Synchrotron Radiation Facility) for providing the beam time.

REFERENCES

1 Yu, G., Gao, J., Hummelen, J.C., Wudl, F. and Heeger, A.J., Science, 1995, 270(5243): 1789
2 Gunes, S., Neugebauer, H. and Sariciftci, N.S., Chem. Rev., 2007, 107(4): 1324
3 Thompson, B.C. and Frechet, J.M.J., Angew. Chem. Int. Ed., 2008, 47(1): 58
4 Chen, J.W. and Cao, Y., Accounts Chem. Res., 2009, 42(11): 1709
5 Henson, Z.B., Mullen, K. and Bazan, G.C., Nat. Chem., 2012, 4(9): 699
6 Li, G., Zhu, R. and Yang, Y., Nat. Photon., 2012, 6(3): 153
7 Li, Y.F., Accounts Chem. Res., 2012, 45(5): 723
8 Ameri, T., Li, N. and Brabec, C.J., Energy Environ. Sci., 2013, 6(8): 2390
9 He, Z.C., Zhong, C.M., Su, S.J., Xu, M., Wu, H.B. and Cao, Y., Nat. Photon., 2012, 6(9): 591
10 You, J.B., Dou, L.T., Yoshimura, K., Kato, T., Ohya, K., Moriarty, T., Emery, K., Chen, C.C., Gao, J., Li, G. and Yang, Y., Nat. Commun., 2013, 4: 1446
11 Chen, C.C., Chang, W.H., Yoshimura, K., Ohya, K., You, J., Gao, J., Hong, Z. and Yang, Y., Adv. Mater., 2014, 26(32): 5670
12 Mayukh, M., Jung, I.H., He, F. and Yu, L.P., J. Polym. Sci., Part B: Polym. Phys., 2012, 50(15): 1057
13 Chen, W., Nikiforov, M.P. and Darling, S.B., Energy Environ. Sci., 2012, 5(8): 8045
14 Chen, L.M., Hong, Z.R., Li, G. and Yang, Y., Adv. Mater., 2009, 21(14-15): 1434
15 Padinger, F., Rittberger, R.S. and Sariciftci, N.S., Adv. Func. Mater., 2003, 13(1): 85
16 Ma, W.L., Yang, C.Y., Gong, X., Lee, K. and Heeger, A.J., Adv. Funct. Mater., 2005, 15(10): 1617
17 Li, G., Shrotriya, V., Huang, J.S., Yao, Y., Moriarty, T., Emery, K. and Yang, Y., Nat. Mater., 2005, 4(11): 864
18 Jin, S.H., Naidu, B.V.K., Jeon, H.S., Park, S.M., Park, J.S., Kim, S.C., Lee, J.W. and Gal, Y.S., Sol. Energy Mater. Sol. Cells., 2007, 91(13): 1187
19 Zhao, Y., Xie, Z.Y., Qu, Y., Geng, Y.H. and Wang, L.X., Appl. Phys. Lett., 2007, 90(4): 043504
20 Peet, J., Kim, J.Y., Coates, N.E., Ma, W.L., Moses, D., Heeger, A.J. and Bazan, G.C., Nat. Mater., 2007, 6(7): 497
21 Huo, L.J., Zhang, S.Q., Guo, X., Xu, F., Li, Y.F. and Hou, J.H., Angew. Chem. Int. Ed., 2011, 50(41): 9697
22 Chen, S., Small, C.E., Amb, C.M., Subbiah, J., Lai, T.H., Tsang, S.W., Manders, J.R., Reynolds, J.R. and So, F., Adv. Energy Mater., 2012, 2(11): 1333
23 Cabanetos, C., El Labban, A., Bartelt, J.A., Douglas, J.D., Mateker, W.R., Frechet, J.M.J., McGehee, M.D. and Beaujuge, P.M., J. Am. Chem. Soc., 2013, 135(12): 4656
24 Chu, T.Y., Lu, J.P., Beaupre, S., Zhang, Y.G., Pouliot, J.R., Wakim, S., Zhou, J.Y., Leclerc, M., Li, Z., Ding, J.F. and Tao, Y., J. Am. Chem. Soc., 2011, 133(12): 4250
25 Liao, H.C., Ho, C.C., Chang, C.Y., Jao, M.H., Darling, S.B. and Su, W.F., Mater. Today, 2013, 16(9): 326
26 Darling, S.B. and You, F.Q., RSC Adv., 2013, 3(39): 17633
27 Chen, F.C., Tseng, H.C. and Ko, C.J., Appl. Phys. Lett., 2008, 92(10): 103316
28 Moule, A.J. and Meerholz, K., Adv. Mater., 2008, 20(2): 240
29 Yao, Y., Hou, J.H., Xu, Z., Li, G. and Yang, Y., Adv. Funct. Mater., 2008, 18(12): 1783
30 Salim, T., Wong, L.H., Brauer, B., Kukreja, R., Foo, Y.L., Bao, Z.N. and Lam, Y.M., J. Mater. Chem., 2011, 21(1): 242
31 Eom, S.H., Park, H., Mujawar, S.H., Yoon, S.C., Kim, S.S., Na, S.I., Kang, S.J., Khim, D., Kim, D.Y. and Lee, S.H., Org. Electron., 2010, 11(9): 1516
32 Park, C.D., Fleetham, T.A., Li, J. and Vogt, B.D., Org. Electron., 2011, 12(9): 1465
33 Li, G., Yao, Y., Yang, H., Shrotriya, V., Yang, G. and Yang, Y., Adv. Funct. Mater., 2007, 17(10): 1636
34 Chen, W.C., Huang, L.Z., Qiao, X.L., Yang, J.B., Yu, B. and Yan, D.H., Org. Electron., 2012, 13(6): 1086
35 Mihailetchi, V.D., Wildeman, J. and Blom, P.W.M., Phys. Rev. Lett., 2005, 94(12): 126602